



LETTER

A foundation model-enhanced CT radiomics signature for the noninvasive assessment of tertiary lymphoid structures and prediction of therapy benefit in gastric cancer

Xianchun Gao^{1*}, Zhe Li^{2*}, Jun Yu^{1*}, Jiangpeng Wei^{3*}, Didi Wen^{4*}, Ning Han¹, Linbin Lu¹, Yongxi Song⁵, Qiong Xiao⁵, Guangtao Wu⁵, Kun Feng⁵, Shibo Wang¹, Zhongyang Zhang¹, Dai Zhang¹, Ling Chen⁶, Zengshan Li⁶, Minwen Zheng⁴, Yong Xia², Yongzhan Nie¹

¹State Key Laboratory of Holistic Integrative Management of Gastrointestinal Cancers, National Clinical Research Center for Digestive Diseases, Xijing Hospital, Fourth Military Medical University, Xi'an 710032, China; ²School of Computer Science and Engineering, Northwestern Polytechnical University, Xi'an 710068, China; ³Department of Digestive Surgery, Xijing Hospital, Fourth Military Medical University, Xi'an 710032, China; ⁴Department of Radiology, Xijing Hospital, Fourth Military Medical University, Xi'an 710032, China; ⁵Department of Surgical Oncology and General Surgery, The First Hospital of China Medical University, Key Laboratory of Precision Diagnosis and Treatment of Gastrointestinal Tumors (China Medical University), Ministry of Education, Shenyang 110100, China; ⁶State Key Laboratory of Holistic Integrative Management of Gastrointestinal Cancers, Department of Pathology, Xijing Hospital and School of Basic Medicine, Fourth Military Medical University, Xi'an 710032, China

Gastric cancer is a highly heterogeneous tumor type whose treatment responses substantially vary across patients. In recent years, biomarkers have shown promise in guiding individualized treatment regimens for gastric cancer, particularly for targeted therapy and immunotherapy¹. Existing biomarkers, including CD8⁺ T-cell infiltration, PD-L1 expression, microsatellite instability, and tumor mutational burden, remain insufficient to reliably stratify patients for chemotherapy or immunotherapy benefit¹⁻³. Therefore, robust, clinically applicable, noninvasive biomarkers are urgently needed to guide perioperative treatment selection.

Tertiary lymphoid structures (TLSs) are ectopic lymphoid aggregates that develop within tumors and adjacent tissues. Mature TLSs, characterized by organized B-cell follicles with germinal centers, have been consistently associated with improved prognosis and enhanced responses to immunotherapy across multiple tumor types, including gastric cancer⁴⁻⁷. However, current TLS assessment relies on the histopathological evaluation of surgical specimens with

hematoxylin–eosin (H&E) staining, with or without immunohistochemistry⁶. Because TLSs are heterogeneously distributed and often sparse, their reliable evaluation typically requires large resection specimens; therefore, this approach is impractical for patients without surgical tissue available preoperatively.

Recent advances in radiomics and foundation model-based representation learning have substantially expanded the biological interpretability of routine computed tomography (CT) imaging, thereby enabling noninvasive inference of molecular and immune microenvironment features⁸. Building on this framework, we developed a foundation model-enhanced CT radiomics signature (FMRS) to noninvasively identify TLS status in gastric cancer, and evaluated its prognostic and predictive value across perioperative treatment settings.

FMRS predicts TLS classification from CT images

For training the CT-based FMRS classification model, this retrospective, multicenter study included 611 patients with stage II–III gastric adenocarcinoma who underwent curative resection and preoperative contrast-enhanced CT at Xijing Hospital between 2015 and 2018 (**Figure 1A**). Patients were randomly assigned to a training cohort ($n = 304$) or an internal validation cohort ($n = 307$) according to a computer-generated random sequence implemented in R software (**Table 1**). TLS maturity in surgical specimens was assessed by experienced

*These authors contributed equally to this work.

Correspondence to: Minwen Zheng, Yong Xia, and Yongzhan Nie
E-mail: zhengmw2007@163.com, yxia@nwpu.edu.cn, and yongznie@fmmu.edu.cn

ORCID ID: <https://orcid.org/0000-0003-1124-4548>

Received January 26, 2026; accepted March 6, 2026;

published online April 16, 2026.

Available at www.cancerbiomed.org

©2026 The Authors. Creative Commons Attribution-NonCommercial 4.0 International License (CC BY-NC 4.0)

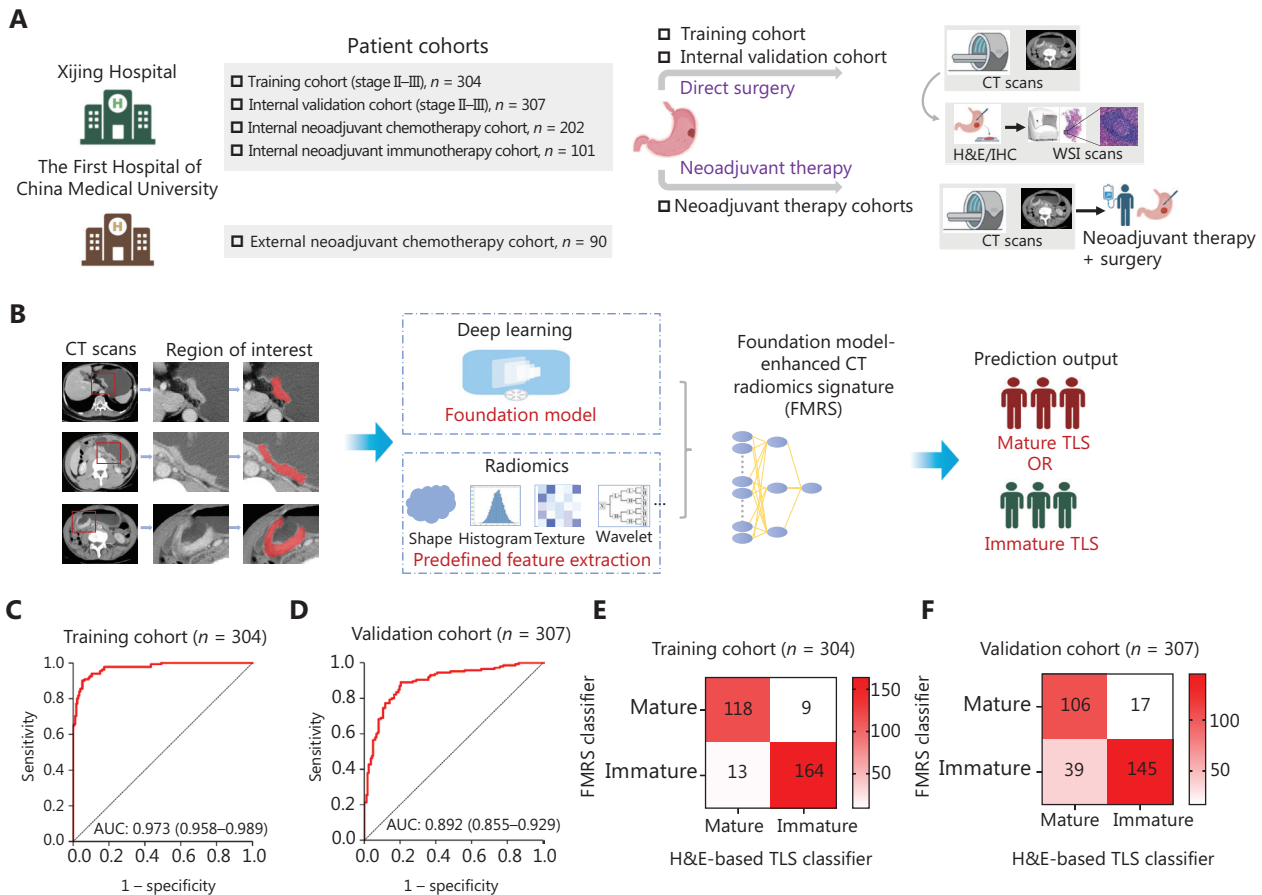


Figure 1 Continued

pathologists using standardized morphological criteria and, when necessary, immunohistochemical staining for CD20, CD21, and CD23 (**Figure S1**). Tumors were classified as TLS-immature (no TLSs or only aggregates) or TLS-mature (primary and/or secondary follicle-like structures).

For evaluation of treatment response, 3 independent neoadjuvant cohorts were enrolled: an internal neoadjuvant chemotherapy cohort ($n = 202$), an internal neoadjuvant anti-PD-1 plus chemotherapy cohort ($n = 101$), and an external neoadjuvant chemotherapy cohort from the First Hospital of China Medical University ($n = 90$) (**Figure 1A** and **Table 1**). All neoadjuvant CT scans were obtained before initiation of neoadjuvant treatment.

Portal venous phase CT images were used for model development. Tumors were manually segmented according to a consensus between 2 radiologists. Deep imaging features were extracted with a pretrained foundation model (FMCIB) trained on more than 11,000 radiographic lesions across multiple anatomical sites⁹. These deep features were integrated with handcrafted radiomic features, thereby yielding a fused high-dimensional representation that was input into a fully connected prediction head to generate a continuous FMRS

score (**Figures 1B** and **S2**). Detailed methods are provided in the **Supplementary material**.

The FMRS demonstrated excellent performance for TLS classification. In the training cohort, the model achieved an area under the receiver operating characteristic curve (AUC) of 0.973 (95% CI, 0.958–0.989) (**Figure 1C**), and similarly strong discrimination was found in the internal validation cohort (AUC, 0.892; 95% CI, 0.855–0.929) (**Figure 1D**). According to an optimal cut-off derived from the training cohort (0.548), patients were stratified into low (immature)- and high (mature)- FMRS groups. As expected, the confusion matrix showed high concordance between model predictions and H&E-defined TLS classification (**Figure 1E** and **1F**).

Prognostic value of FMRS for overall survival (OS) and disease-free survival (DFS)

High FMRS was strongly associated with favorable prognosis. In the training cohort, patients with high FMRS exhibited

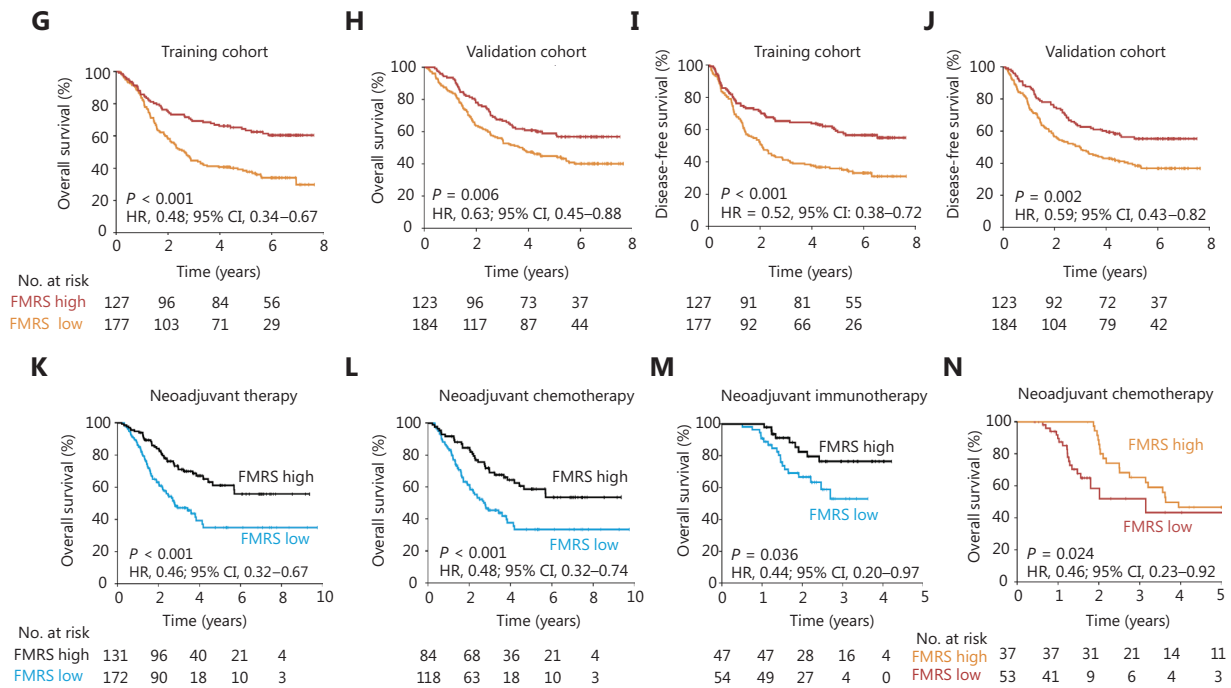


Figure 1 Development, validation, and clinical utility of the FMRS for TLS prediction and survival stratification. (A) Overview of the study workflow, including patient selection, data collection, and cohort allocation. (B) Schematic illustration of the CT-based framework for predicting TLS status with the foundation model-enhanced radiomics signature (FMRS). (C, D) Receiver operating characteristic (ROC) curves demonstrating FMRS performance for TLS classification in the training cohort (C) and validation cohort (D). (E, F) Confusion matrices showing agreement between FMRS-predicted TLS status and histopathological assessment in the training cohort (E) and validation cohort (F); correctly classified cases are shown along the diagonal, and misclassifications are shown off the diagonal. (G–J) Kaplan–Meier survival analyses, stratified by FMRS status: overall survival (OS) in the training cohort (G) and validation cohort (H), and disease-free survival (DFS) in the training cohort (I) and validation cohort (J). (K–M) Kaplan–Meier curves for OS, comparing FMRS-high and FMRS-low groups in the internal neoadjuvant therapy cohorts: all patients (K), neoadjuvant chemotherapy subgroup (L), and neoadjuvant immunotherapy subgroup (M). (N) Kaplan–Meier analysis of OS according to FMRS status in the external neoadjuvant chemotherapy validation cohort. AUC, area under the curve; FMRS, foundation model-enhanced CT radiomics signature; H&E, hematoxylin–eosin staining; HR, hazard ratio; IHC, immunohistochemistry; TLS, tertiary lymphoid structure; WSI, whole slide scanning.

significantly greater OS and DFS than patients with low FMRS (5-year OS, 70.4% vs. 40.1%, $P < 0.001$; 5-year DFS, 64.7% vs. 36.5%, $P < 0.001$) (**Figure 1G and 1I**). These findings were independently validated in the internal validation cohort (**Figure 1H and 1J**). Time-dependent AUC analyses indicated that FMRS maintained consistent predictive performance across 1–5 years after surgery in both the training and internal validation cohorts (**Figure S3**). Multivariable Cox regression analyses confirmed FMRS as an independent prognostic factor for outcomes (**Tables S1 and S2**).

FMRS as a predictive biomarker of benefit from adjuvant chemotherapy

Beyond prognostic stratification, FMRS predicted the benefit from adjuvant chemotherapy. Among patients receiving

postoperative chemotherapy, patients with high FMRS derived significantly greater survival benefit than patients with low FMRS, and a significant interaction was observed between FMRS status and treatment (OS: $P = 0.003$ for the interaction; DFS: $P = 0.004$ for the interaction) (**Figure S4**). These results remained consistent across tumor stage subgroups; therefore, FMRS might serve as a predictive biomarker for chemotherapy responsiveness (**Figure S5**).

FMRS status predicts response and survival benefit from neoadjuvant therapy

The clinical utility of FMRS was evaluated in 3 neoadjuvant cohorts, including 2 internal cohorts (neoadjuvant chemotherapy and anti-PD-1 plus chemotherapy) and 1 external

Table 1 Baseline characteristics of patients in the training, internal, and external validation cohorts

Characteristic	Patients, No. (%)			
	Training cohort (<i>n</i> = 304)	Internal validation cohort (<i>n</i> = 307)	Internal neoadjuvant therapy cohort (<i>n</i> = 303)	External neoadjuvant chemotherapy cohort (<i>n</i> = 90)
Age, mean (SD), y	59.4 (10.2)	59.0 (9.6)	60.4 (8.9)	59.2 (10.1)
Sex				
Male	226 (74.3)	250 (81.4)	249 (82.2)	64 (71.1)
Female	78 (25.7)	57 (18.6)	54 (17.8)	26 (28.9)
CEA, ng/mL				
<5	234 (77.0)	250 (81.4)	198 (65.3)	61 (67.8)
≥5	70 (23.0)	57 (18.6)	105 (34.7)	29 (32.2)
CA 19-9, U/mL				
<37	229 (75.3)	234 (76.2)	230 (75.9)	64 (71.1)
≥37	75 (24.7)	73 (23.8)	73 (24.1)	26 (28.9)
Primary tumor location				
Proximal	102 (33.6)	104 (33.9)	139 (45.9)	21 (23.3)
Body	72 (23.7)	72 (23.5)	82 (27.1)	25 (27.8)
Antrum	130 (42.8)	131 (42.7)	82 (27.1)	44 (48.9)
Pathologic T stage				
pT1–2	26 (8.6)	36 (11.7)	—	—
pT3–4	278 (91.4)	271 (88.3)	—	—
Pathologic N stage				
pN0–1	106 (34.9)	105 (34.2)	—	—
pN2–3	198 (65.1)	202 (65.8)	—	—
Pathologic TNM stage				
pStage II	85 (28.0)	96 (31.3)	—	—
pStage III	219 (72.0)	211 (68.7)	—	—
Neoadjuvant therapy				
Chemotherapy	—	—	202 (66.7)	90 (100)
Immunotherapy	—	—	101 (33.3)	0 (0)
Adjuvant chemotherapy				
No	54 (17.8)	52 (16.9)	—	—
Yes	250 (82.2)	255 (83.1)	—	—
TRG				
0	—	—	33 (10.9)	6 (6.7)
1	—	—	36 (11.9)	13 (14.4)
2	—	—	112 (37.0)	30 (33.3)

Table 1 Continued

Characteristic	Patients, No. (%)			
	Training cohort (<i>n</i> = 304)	Internal validation cohort (<i>n</i> = 307)	Internal neoadjuvant therapy cohort (<i>n</i> = 303)	External neoadjuvant chemotherapy cohort (<i>n</i> = 90)
3	—	—	122 (40.3)	41 (45.6)
TLS class				
Immature TLS	173 (56.9)	162 (52.8)	—	—
Mature TLS	131 (43.1)	145 (47.2)	—	—

No, number; SD, standard deviation; TRG, tumor regression grade; TLS, tertiary lymphoid structure.

neoadjuvant chemotherapy cohort. Across the internal neoadjuvant cohorts (*n* = 303), the overall pathological response rate (TRG 0/1) was 22.8%. Patients with high FMRS achieved significantly higher response rates than patients with low FMRS (31.3% vs. 16.3%, *P* = 0.002) (Figure S6A) and demonstrated superior OS (hazard ratio, 0.46; 95% CI, 0.32–0.67; *P* < 0.001) (Figure 1K).

Among patients receiving neoadjuvant chemotherapy alone (*n* = 202), higher FMRS was associated with greater pathological response (22.6% vs. 11.0%, *P* = 0.026) (Figure S6B) and longer OS (*P* < 0.001) (Figure 1L). These findings were independently validated in the external cohort, in which higher FMRS predicted longer OS (*P* = 0.024) and higher 3-year OS (65.2% vs. 50.3%) (Figure 1N).

In the neoadjuvant anti-PD-1-based cohort (*n* = 101), high FMRS was strongly associated with pathological response (46.8% vs. 27.8%, *P* = 0.048) (Figure S6C) and prolonged OS (*P* = 0.036) (Figure 1M). FMRS demonstrated a predictive performance comparable to that of the combined positive score (CPS) of PD-L1 expression (AUC, 0.602 vs. 0.635; *P* = 0.661). A combined model incorporating clinical stage, CPS, and FMRS further increased predictive accuracy for immunotherapy response (AUC, 0.709) (Figure S6D).

The biological plausibility of these findings is supported by known associations among TLS maturity, immune cell infiltration, and tumor vascular remodeling. Mature TLSs, characterized by dense lymphocyte aggregates, germinal centers, and high endothelial venules, are expected to influence tumor morphology and heterogeneity detectable on CT imaging^{6,10}. By integrating deep semantic features with quantitative radiomics, the FMRS captures these complex microenvironmental signatures in a noninvasive manner.

The retrospective nature of this study introduced potential for selection bias. In addition, the subgroup analyses were exploratory and were not adjusted for multiple comparisons. Our findings should therefore be interpreted with caution. Although interaction analyses suggested a modification effect of FMRS on treatment benefit, the modest subgroup sample

sizes in some strata might have diminished the precision and stability of the interaction estimates. Model uncertainty was partly reflected by 95% confidence intervals for major performance estimates, including AUCs and hazard ratios, as well as by evaluation in independent internal and external validation cohorts. However, bootstrap-based or repeated cross-validation procedures were not performed, thus potentially limiting the precision of model stability assessment. Therefore, our results require further confirmation in prospective, adequately powered, multicenter studies and randomized clinical trials to validate the clinical utility, reproducibility, and generalizability of the FMRS for TLS assessment and treatment benefit prediction.

In conclusion, we present a FMRS that enables noninvasive assessment of TLS status in gastric cancer. The FMRS independently predicts prognosis and identifies patients likely to benefit from adjuvant chemotherapy and neoadjuvant chemoimmunotherapy. This approach offers a practical imaging-based strategy for immune microenvironment assessment and may facilitate personalized perioperative treatment selection in patients with gastric cancer. Future studies are warranted to validate the FMRS across diverse populations and standardized imaging protocols, to facilitate its potential integration into clinical decision-making.

Grant support

This work was supported by the National Natural Science Foundation of China (Grant No. 82202837), the Noncommunicable Chronic Diseases-National Science and Technology Major Project (Grant Nos. 2025ZD0545200, and 2023ZD0501400), the National Natural Science Foundation of China (Grant Nos. 82421002 and 82350122), the National Key R&D Program of China (Grant No. 2022YFC2505100), the Postdoctoral Fellowship Program of CPSF (Grant No. GZC20242251), and the China Postdoctoral Science Foundation (Grant No. 2024M754223).

Conflict of interest statement

No potential conflicts of interest are disclosed.

Author contributions

Concept and design: Nie, Xia, and Zheng.

Acquisition, analysis, or interpretation of data: All authors.

Drafting of the manuscript: Gao, Zhe Li, Yu, and Wei.

Critical revision of the manuscript for important intellectual content: Nie, Xia, and Zheng.

Statistical analysis: Gao, Zhe Li, Yu, and Zheng.

Funding acquisition: Nie and Gao.

Administrative, technical, or material support: Xia.

Supervision: Nie, Xia, and Zheng.

Data availability statement

The data generated in this study are available upon request from the corresponding authors.

References

- Sundar R, Nakayama I, Markar SR, Shitara K, van Laarhoven HWM, Janjigian YY, et al. Gastric cancer. *Lancet*. 2025; 405: 2087-102.
- Verschoor YL, van de Haar J, van den Berg JG, van Sandick JW, Kodach LL, van Dieren JM, et al. Neoadjuvant atezolizumab plus chemotherapy in gastric and gastroesophageal junction adenocarcinoma: the phase 2 PANDA trial. *Nat Med*. 2024; 30: 519-30.
- Chong X, Madeti Y, Cai J, Li W, Cong L, Lu J, et al. Recent developments in immunotherapy for gastrointestinal tract cancers. *J Hematol Oncol*. 2024; 17: 65.
- Vanhersecke L, Brunet M, Guegan JP, Rey C, Bougouin A, Cousin S, et al. Mature tertiary lymphoid structures predict immune checkpoint inhibitor efficacy in solid tumors independently of PD-L1 expression. *Nat Cancer*. 2021; 2: 794-802.
- Li Z, Jiang Y, Li B, Han Z, Shen J, Xia Y, et al. Development and validation of a machine learning model for detection and classification of tertiary lymphoid structures in gastrointestinal cancers. *JAMA Netw Open*. 2023; 6: e2252553.
- Deng S, Chen Y, Song B, Wang H, Huang S, Wu K, et al. Tertiary lymphoid structures in cancer: spatiotemporal heterogeneity, immune orchestration, and translational opportunities. *J Hematol Oncol*. 2025; 18: 97.
- Chen Y, Sun Z, Yin J, Ahmad MU, Zhou Z, Feng W, et al. Digital assessment of tertiary lymphoid structures and therapeutic responses in gastric cancer: a multicentric retrospective study. *Int J Surg*. 2024; 110: 6732-47.
- Niu C, Lyu Q, Carothers CD, Kaviani P, Tan J, Yan P, et al. Medical multimodal multitask foundation model for lung cancer screening. *Nat Commun*. 2025; 16: 1523.
- Pai S, Bontempi D, Hadzic I, Prudente V, Sokac M, Chaunzwa TL, et al. Foundation model for cancer imaging biomarkers. *Nat Mach Intell*. 2024; 6: 354-67.
- Su JY, Li JR, Pan LX, Ma YL, Tian W, Jiang YM, et al. Tertiary lymphoid structures in HCC: Influence on immune cell profiles in tumors and on efficacy of adjuvant PD-1 inhibitor therapy after hepatectomy. *Hepatology*. 2025.

Cite this article as: Gao X, Li Z, Yu J, Wei J, Wen D, Han N, et al. A foundation model-enhanced CT radiomics signature for the noninvasive assessment of tertiary lymphoid structures and prediction of therapy benefit in gastric cancer. *Cancer Biol Med*. 2026; x: xx-xx. doi: 10.20892/j.issn.2095-3941.2026.0076